

Mechanical Behavior of Polymer Microlayers

Julia Kerns¹, Alex Hsieh², Anne Hiltner^{1*} and Eric Baer¹

¹ Department of Macromolecular Science and Center for Applied Polymer Research, Case Western Reserve University, Cleveland, OH 44106-7202, U.S.A.

² Army Research Laboratory, Aberdeen Proving Ground, MD 21005-5069, U.S.A.

SUMMARY: The mechanical behavior of polycarbonate (PC) coextruded as microlayers with a brittle polymer, either poly(styrene-*co*-acrylonitrile) (SAN) or poly(methyl methacrylate) (PMMA), was examined. Adhesion between layers was measured with the T-peel method. The much higher interfacial toughness of PC/PMMA microlayers compared to PC/SAN was attributed to partial miscibility. Comparison of the microdeformation behavior of 32-layer PC/SAN and PC/PMMA microlayers revealed that very good adhesion between PC and PMMA constrained yielding of the PC. This was seen in the tensile stress-strain curves as a broader stress drop at the yield point and a lower fracture strain. Decreasing the layer thickness by increasing the number of layers enhanced the ductility of both PC/SAN and PC/PMMA microlayers. A PC/PMMA microlayer with 4096 layers and a composition of 80 % PC achieved the ballistic performance of polycarbonate.

Introduction

Coextrusion is one way in which two or more polymers can be physically combined for the purpose of achieving improved properties.¹ Previous studies of microlayers with many alternating layers of polycarbonate (PC) and poly(styrene-*co*-acrylonitrile) (SAN) showed that when the layer thickness decreased to the micron scale, the toughness and impact resistance of these microlayers was enhanced. The increase in toughness was due to a change in the deformation mechanism of the SAN layers from crazing to cooperative shear yielding with PC. This was only possible because the adhesion between PC and SAN was good enough to ensure stress transfer across the PC/SAN interface during deformation.

To determine the PC/SAN adhesive strength, the T-peel method was used to delaminate microlayers. A strong effect of layer thickness on delamination toughness of PC/SAN microlayers was found^{2,3}. With SAN layers thinner than 1.5 μm and PC layers thicker than 1.7 μm , the crack propagated along a single interface; damage in front of the crack tip was minimal and the peel toughness of 90 J/m² corresponded to the interfacial toughness.² Thicker SAN layers crazed. However, interfacial failure between PC and SAN could also occur at very slow peel rates, regardless of the layer thickness.^{2,3}

Combining poly(methyl methacrylate) (PMMA) with PC is attractive because PMMA is environmentally resistant and transparent. Microlayering PC and PMMA may achieve the advantages of PMMA without sacrificing toughness. Because PC and PMMA are known to be partially miscible⁴, good adhesion between PC and PMMA is expected.

This paper compares the mechanical behavior of PC/SAN and PC/PMMA microlayers including the effects of layer thickness. The mechanical properties of 32-layer sheets of alternating PC and SAN and alternating PC and PMMA were examined. Microdeformation studies were also carried out on the 32-layer sheets using the optical microscope to examine the irreversible microdeformation processes and the role of interfacial adhesion.

Experimental

The PC was Calibre™ (The Dow Chemical Company, Midland) 300-15 and the PMMA was V826-100 (Ato-Haas, Chicago). The SAN was Tyril™ 867-B (The Dow Chemical Company, Midland). The SAN composition, 25 % acrylonitrile, was chosen for maximum adhesion to PC.⁵

Microlayers of PC/PMMA and PC/SAN with 32, 256, 1024, 2048, and 4096 layers were coextruded with the two-component microlayer system described previously.⁶ The composition was varied by changing the flow rate. The sheets were approximately 1 mm thick and 80 mm wide.

A possible layer thickness dependence was considered when microlayering PC and PMMA for adhesion measurements. The PC/PMMA microlayer used for peel testing had 257 layers, a composition of 90 % PC and 10 % PMMA, and nominal layer thicknesses of 4.0 μm and 0.4 μm . The PC/SAN microlayer had 1857 layers, a composition of 85 % PC and 15 % SAN, and nominal layer thicknesses of 2.5 μm and 0.5 μm . This PC/SAN microlayer was supplied by The Dow Chemical Company.

Tensile specimens were machined from the coextruded sheet parallel to the extrusion direction using a waisted geometry to localize deformation. The grip separation was 55 mm and the width gradually decreased from 30 mm at the grips to 7 mm at the midpoint. Tests were performed on an Instron testing machine at a rate of 0.3 mm/min. At least three specimens of each composition were tested.

Specimens for optical microscopy were prepared by cutting a rectangular strip out of the center of the microlayer with a diamond blade. This resulted in a rectangular specimen between 0.8 and 1.2 mm thick. The cut specimens were polished on a

metallurgical wheel using fine sandpaper and aqueous suspensions of aluminum oxide. The central part of the specimen was thinned to between 0.4 and 0.6 mm to localize the deformation to this region. The polished sample was clamped in a Polymer Laboratories Minimat microtensile tester for uniaxial tensile testing. The microtensile tester was mounted on the stage of an Olympus BH2 optical microscope so that the deformation process could be photographed.⁷ The specimens were stretched at a speed of 0.01 mm/min.

Delamination was carried out with the T-peel test (ASTM D1876). Specimens between 8 and 15 mm wide were notched by pushing a fresh razor blade into the midplane of the sheet.⁸ Specimens were loaded at a rate of 2 mm/min. Some tests were interrupted and the crack tip region was sectioned perpendicular to the plane of the crack with a low-speed diamond saw (Isomet, Bueller Ltd.). The sections were polished on a metallurgical wheel with wet sandpaper and aqueous suspensions of aluminum oxide. The sections were photographed in a transmission optical microscope. Sections of the fracture surface were coated with 100 Å of gold for examination in a JEOL JSM 840A scanning electron microscope.

Results and Discussion

Delamination of Microlayers

Figure 1 shows peel curves for PC/PMMA ($4.0\ \mu\text{m}/0.4\ \mu\text{m}$) and PC/SAN ($2.5\ \mu\text{m}/0.5\ \mu\text{m}$) tested at an extension rate of 2 mm/min.

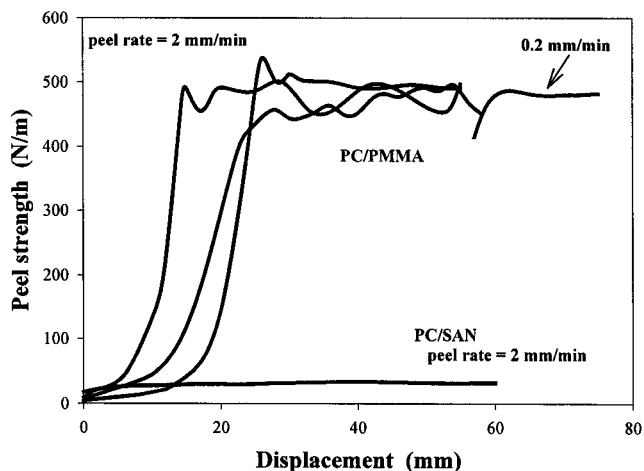


Figure 1 Normalized peel curves of PC/SAN ($2.5\ \mu\text{m}/0.5\ \mu\text{m}$) and PC/PMMA ($4.0\ \mu\text{m}/0.4\ \mu\text{m}$)

A much higher force was required to propagate a delamination crack in PC/PMMA than in PC/SAN. In PC/SAN, the curvature of the arms in the T-peel configuration conformed to the elastic shape⁹, and the arms recovered fully to the original shape after testing. In comparison, the curvature of the PC/PMMA arms was much sharper than the elastica prediction, and the arms remained bent after the test was complete. The permanent deformation in the beam arms was not accounted for in the peel curves shown.

The delamination toughness was calculated as $G = 2P_{cr}/W$ for a specimen of width W , where P_{cr} is the load at which the crack propagated. The PC/SAN failed interfacially with a delamination toughness of 70 J/m^2 . This is comparable to the value of 90 J/m^2 reported previously.² The PC/PMMA had a much higher delamination toughness of 950 J/m^2 .

The PC/PMMA ($4.0 \text{ } \mu\text{m}/0.4 \text{ } \mu\text{m}$) was microlayered with thick PC layers and thin PMMA layers in anticipation that it would fail interfacially. Figure 2 shows the crack tip of a PC/PMMA peel specimen. The crack propagated along a single interface with no evidence of a damage zone at the crack tip.

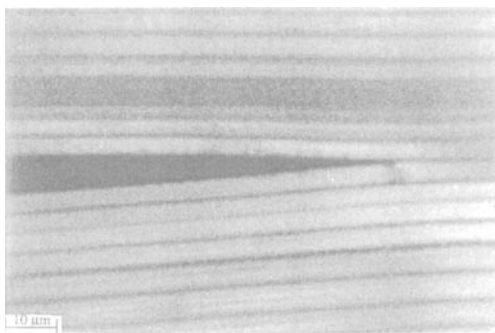


Figure 2
Crack tip of PC/PMMA ($4.0 \text{ } \mu\text{m}/0.4 \text{ } \mu\text{m}$)

Figure 3 shows matching peel surfaces of PC/PMMA ($4.0 \text{ } \mu\text{m}/0.4 \text{ } \mu\text{m}$). Crazing was not observed on the peel surfaces, and there was no evidence that the crack propagated through a layer from one interface to another. Both peel surfaces had a rough texture with wrinkles perpendicular to the peel direction. These features were consistent with the appearance of the crack tip and confirmed an interfacial delamination mechanism. Furthermore, during one of the peel tests of PC/PMMA, the peel rate was decreased to 0.2 mm/min . The peel strength remained the same, which is characteristic of interfacial failure. High peel strength of PC/PMMA is consistent with the partial miscibility of PC and PMMA.⁴

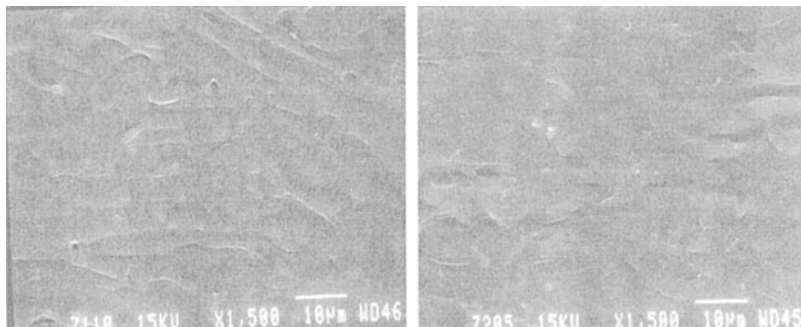


Figure 3 Matching peel surfaces for PC/PMMA ($4.0\ \mu\text{m}/0.4\ \mu\text{m}$)

Deformation of Microlayers with Thick layers

Figure 4 compares stress-strain curves of PC/PMMA (70 %/30 %) and PC/SAN (70 %/30 %) with 32 layers. The slight differences in layer thicknesses originated from a difference in the total thickness of the sample. The PC/SAN yielded at a strain of 6 % and a stress of 65 MPa. As the sample began to neck, there was a sharp stress drop that took place over a strain increment of less than 0.5 %. The PC/SAN fractured at about 60 % strain. The PC/PMMA with the same number of layers and same composition yielded at a slightly higher strain of 7 % and a stress of 62 MPa. The stress drop associated with yielding occurred over a 2 % strain increment in PC/PMMA, which was more gradual than in PC/SAN. The PC/PMMA fractured at about 44 % strain, slightly lower than the PC/SAN.

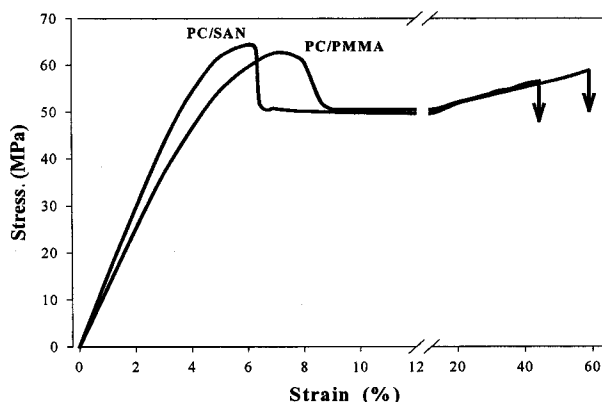


Figure 4 Stress-strain curves of PC/SAN ($15\ \mu\text{m}/6\ \mu\text{m}$) and PC/PMMA ($27\ \mu\text{m}/11\ \mu\text{m}$)

The effect of composition on the stress-strain curve of PC/PMMA with 32 layers is seen in Figure 5. With increasing PMMA content, the yield stress did not change. However,

the yield region broadened. The strain increment over which the stress drop occurred increased from 2 to 3 % as the PMMA content increased from 30 to 60 %. All the samples were ductile; however, the fracture strain decreased with increasing PMMA content.

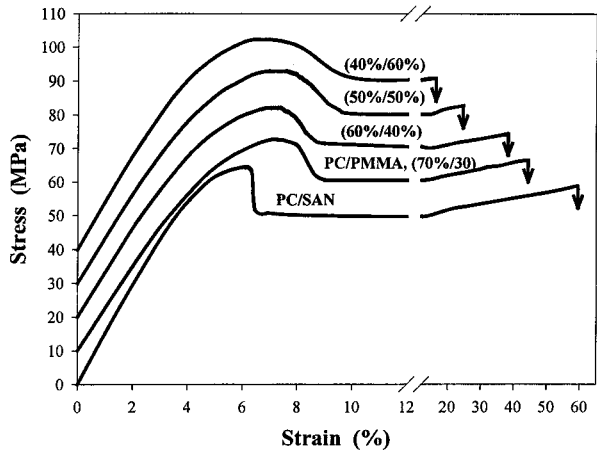


Figure 5 Stress-strain curves for 32-layer PC/PMMA samples at various compositions; curves are shifted vertically by 10 MPa

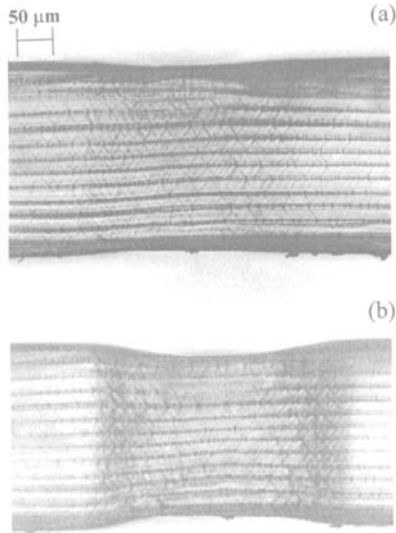


Figure 6
Optical micrographs of 32-layer PC/SAN (15 μm/6 μm) microlayers: (a) 6.0 % strain, (b) 6.5 % strain

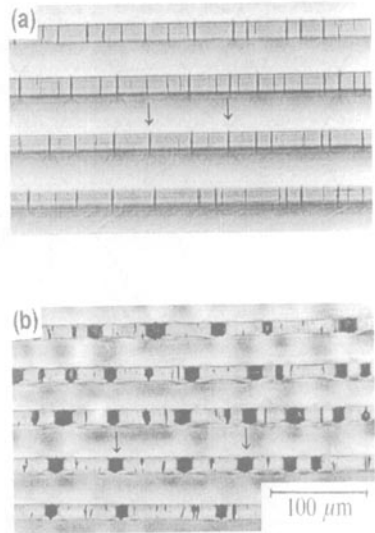


Figure 7
Optical micrographs of 49-layer PC/SAN (29 μm/16 μm): (a) before necking, and (b) the same region after necking. The arrows identify the same two crazes in both micrographs.¹⁰

Differences in the yielding behavior of PC/SAN and PC/PMMA microlayers were studied further by examining the microdeformation mechanisms. Figure 6 shows the microdeformation behavior of PC/SAN (70 %/30 %) during formation of the neck at a strain rate of 0.01 mm/min. The first mechanism observed was the formation of crazes in

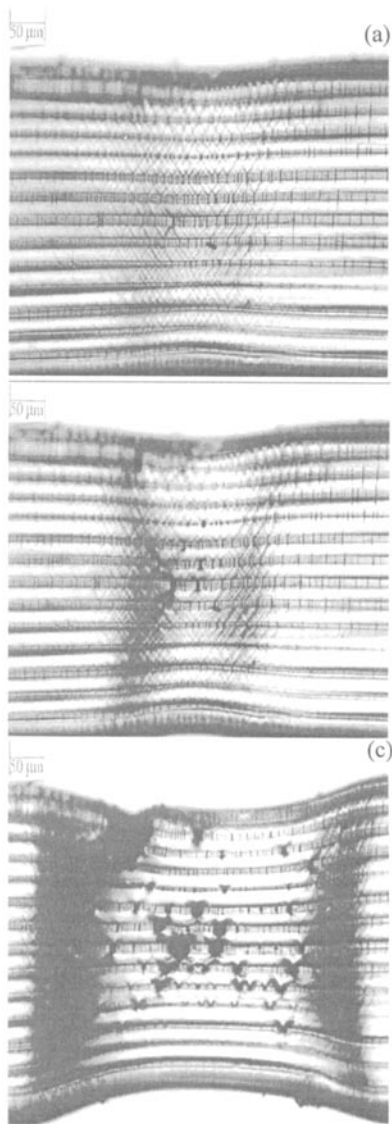


Figure 8 Optical micrographs of 32-layer PC/PMMA (27 μm /11 μm): (a) 7.0 % strain, (b) 7.5 % strain, (c) 9.0 % strain

the SAN layers. Due to good adhesion between PC and SAN, shearbands initiated in PC at the stress concentrations created by the craze tips. At the yield point, shearbands coalesced and crazes opened up into cracks. The large cracks did not prevent the PC/SAN from forming a stable neck (Figure 7).¹⁰ As the PC layers drew, SAN layers formed large holes. Apparently, the interface was sufficiently adaptable that at high strains, the PC layers could draw more or less independently of the SAN layers. High strains were achieved before fracture occurred.

Figure 8 shows the microdeformation behavior of PC/PMMA (70 %/30 %) during formation of the neck at a strain rate of 0.01 mm/min. Initially, the deformation closely resembled that of PC/SAN. The first deformation mechanism observed was crazing in the PMMA layers. With increasing strain, shearbands initiated from the craze tips in the PC layers. However, as necking started and the shearbands in PC coalesced, the crazes in PMMA resisted opening up into cracks. As a result, yielding, as indicated by the formation of a well-defined neck, occurred at a higher strain in PC/PMMA than in PC/SAN (compare Fig. 6b at 6.5 % strain with Fig.

8c at 9.0 % strain). As the neck formed, the PC layers started to draw as cracks opened up in the PMMA layers. However, drawing of the PC layers was constrained by the PMMA layers because of the very good adhesion between PC and PMMA. Apparently, the PC/PMMA interface remained firmly intact during formation of the neck. Cracks opening up in the PMMA layers extended into the PC layers. When one of the cracks reached a critical size, the specimen fractured.

The microdeformation behavior explained the differences in stress-strain behavior of PC/PMMA and PC/SAN. The higher yield strain and broader stress drop associated with yielding of PC/PMMA were due to constraints on yielding and drawing of PC imposed by the PMMA layers. Very strong adhesion of PC and PMMA layers prevented PMMA crazes from opening up into large cracks which was the mechanism by which SAN accommodated the high strain in the neck of the PC/SAN microlayer.

Deformation of Microlayers with Thin Layers

Previous studies found that with increasing number of layers, the ductility of PC/SAN microlayers increases. This phenomenon is illustrated in Figure 9 which shows the effect of layer thickness on the impact strength of PC/SAN microlayers.¹¹ For example, the relative impact strength of a 50/50 composition increases from less than 0.1 to almost 1.0 as the number of layers increases from 3 to 391. This is due to the onset of cooperative deformation as the layers become thinner.

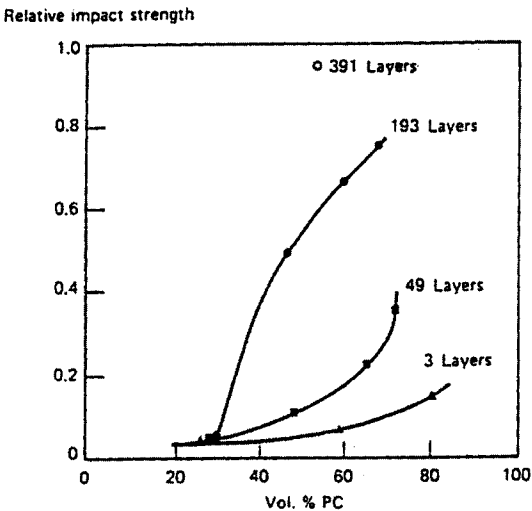


Figure 9
Relative impact strength at room temperature of PC/SAN sheet as a function of PC content and number of layers (relative impact strength of PC=1.0 and SAN = 0.0).¹¹

Figure 10 illustrates the microdeformation behavior of a PC/SAN microlayer with thin layers before and after necking.¹² Before yielding, crazes formed and shearbands initiated at the craze tips (Figure 10a). The adhesion was good enough between PC and SAN so that when shearbands formed, they grew across the PC layers and extended into the SAN layers. Figure 10b shows the sample after necking. The SAN crazes remained closed as both PC and SAN layers yielded and drew out. This accounted for the increase in toughness seen with increasing number of layers.

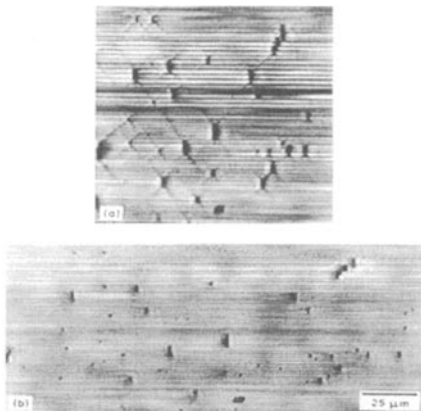


Figure 10

Optical micrographs showing microdeformation of the 776-layer PC/SAN microlayer deformed parallel to the extrusion direction: the same region is shown (a) before necking and (b) after necking.¹²

Figure 11 shows the effect of layer thickness on the stress-strain curve of PC/PMMA (70 %/30 %). The shape of the yield region was not affected. However, greater ductility with higher number of layers was indicated by the increase in fracture strain from 44 to 86 %.

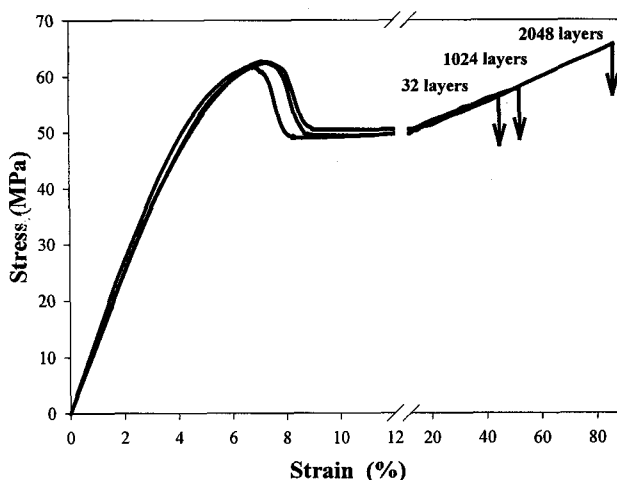


Figure 11 Stress-strain curves of PC/PMMA with 32, 1024, and 2048 layers

Another example of the layer thickness effect is shown in Figure 12, which compares the ballistic properties of PC/PMMA (80 %/20 %) microlayers with the PC control. In the PC control, the bullet did not pass through the specimen. Dissipation of the energy from the impact created an impression where the specimen was clamped, seen by the circular mark on the border of the test area. In contrast, the bullet passed through the 256-layer microlayer without dissipating enough energy to produce a clamp mark. The 1024-layer specimen fractured, but some energy was absorbed by the specimen as seen by the circular crack near the position of the clamp. The microlayer with 2048 layers also cracked. However, this specimen absorbed the impact energy because the bullet did not pass through the specimen and a clamp mark was clearly visible. The 4096-layer specimen resembled the PC control. No fracture occurred, although this sample contained 20 % PMMA. The marking from the clamp ring indicated that the energy was distributed throughout the specimen.

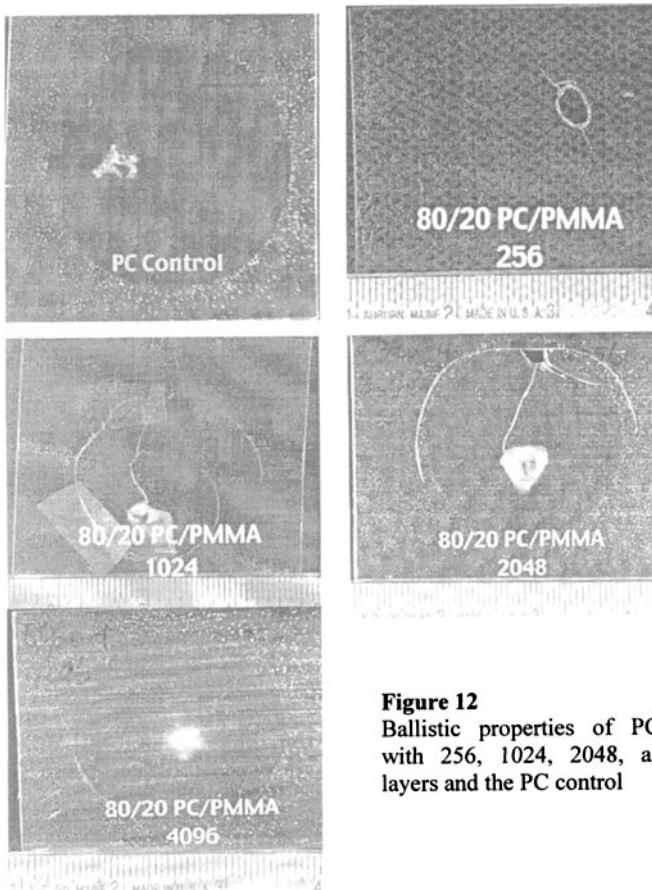


Figure 12
Ballistic properties of PC/PMMA
with 256, 1024, 2048, and 4096
layers and the PC control

Conclusions

1. The delamination toughness of PC/PMMA (4.0 $\mu\text{m}/0.4 \mu\text{m}$) is considerably higher than the delamination toughness of PC/SAN (2.5 $\mu\text{m}/0.5 \mu\text{m}$). This difference is attributed to partial miscibility of PC and PMMA.
2. Very good adhesion between PC and PMMA constrains yielding of the PC in microlayers with thick layers. As a result, PC/PMMA microlayers have a broader stress drop at the yield point and a lower fracture strain than PC/SAN with thick layers.
3. In both PC/PMMA and PC/SAN microlayers, decreasing layer thickness is accompanied by an increase in ductility. With decreasing layer thickness, the ballistic properties of PC/PMMA (80 %/20 %) microlayers improve so that with 4096 layers, the microlayer resembles the PC control in ballistic performance.

Acknowledgements

This work was generously supported by the Army Research Office (grant DAAG55-98-1-0311) and the National Science Foundation (grant DMR97-05696).

References

- ¹ B.L. Gregory, A. Siegmann, J. Im, A. Hiltner and E. Baer, *J. Mater. Sci.* **22**, 532 (1987)
- ² A. Hiltner, T. Ebeling, A. Shah, C. Mueller and E. Baer, *Interfacial Aspects of Multicomponent Polymer Materials*, D.J. Lohse, T.P. Russell and L.H. Sperling, Eds, Plenum, New York 1997, p. 95
- ³ C. Mueller, S. Nazarenko, T. Ebeling, T. Schuman, A. Hiltner and E. Baer, *Polym. Eng. Sci.* **37**, 355 (1997)
- ⁴ W. N. Kim and C.M. Burns, *Macromolecules* **20**, 1876 (1987)
- ⁵ J.D. Keitz, J.W. Barlow and D.R. Paul, *J. Appl. Polym. Sci.*, **29**, 3131 (1984)
- ⁶ C. Mueller, J. Kerns, T. Ebeling, S. Nazerenko, A. Hiltner and E. Baer, *Polymer Process Engineering 97*, P.D. Coates, Ed., University Press, Cambridge 1997, p. 137
- ⁷ D. Haderski, K. Sung, J. Im, A. Hiltner and E. Baer, *J. Appl. Polym. Sci.* **52**, 121 (1994)
- ⁸ T. Ebeling, A. Hiltner and E. Baer, *J. Appl. Polym. Sci.* **68**, 793 (1998)
- ⁹ K. Kendall, *J. Adhes.* **5**, 105 (1973)
- ¹⁰ K. Sung, D. Haderski, A. Hiltner and E. Baer, *J. Appl. Polym. Sci.* **52**, 147 (1994)
- ¹¹ J. Im, E. Baer and A. Hiltner, *High Performance Polymers*, E. Baer and A. Moet, Eds., Hanser Verlag, Munich 1991, p. 175
- ¹² M. Ma, K. Vijayan, A. Hiltner and E. Baer, *J. Mater. Sci.* **25**, 2039 (1990)